Open Access Journal

Journal of Power Technologies 97 (4) (2017) 314–326

journal homepage:papers.itc.pw.edu.pl

Numerical calculation of rotating detonation chamber

Zhenda Shi, Jan Kindracki*

Institute of Heat Engineering, Warsaw University of Technology, 21/25 Nowowiejska Street, 00-665 Warsaw, Poland

Abstract

ANSYS FLUENT 14 supplied the CFD tools used in the numerical calculation of rotating detonation combustion. During calculations, various fuel injection methods and configurations of combustion chamber were applied in an attempt to obtain stable and correct detonation propagation results in a separated fuel-air injection system (non-premixed combustion model). However, FLUENT was not originally designed for detonation combustion and the failure to achieve re-initiation of detonation after collision was always the core issue in the non-premixed combustion model. Thus, this paper mainly focuses on research into the behavior of stable continuously rotating detonation in premixed combustion cases. The analysis of stable continuously rotating detonation behaviors and structures was carried out with different boundary conditions and mesh cells. The pressures were measured by using a number of artificial sensors inserted near the chamber outside surface in various axial and/or circumferential directions. With those key results in the case of premixed combustion, we were able to comparably conclude that stable rotating detonation would also be generated if the refilling process were properly exhibited in non-premixed combustion. The paper finishes with evaluations and conclusions regarding general detonation behaviors and performances.

Keywords: Rotating detonation engine; premixed/non-premixed combustion; 2D/3D chamber model

1. Introduction

Detonation is one of two main kinds of combustion and could be expressed as a complex phenomenon consisting of a shock wave and combustion zone. The shock wave triggers an exothermic reaction by compressing the fresh mixture (increasing pressure and temperature) shortly after ignition and the combustion zone releases the energy that supports the shock wave in continuously propagating forward. This type of combustion gains extra working energy through dramatically increased pressure after the detonation wave. The first official description of detonation was made public by Erthelot, Vieille, Mallard and Le Chatelier in 1881. A couple of decades later, Chapman and Jouguet presented a zero dimensional theory of detonation [1, 2]. Vojciechovski, Metrofanov and Topchiyan demonstrated continuously rotating detonation about a half century later [3]. The first successful attempt at applying pulse detonation to jet propulsion was in 1950s, by Nicholls [4]. In 2004, Tobita, Fujiwara and Wolanski applied for a patent on the rotating detonation engine and the patent was issued in 2005 [5]. Bykovskii et al. [6–8], Bykovskii and Vedernikov [9] published pictures of a velocity compensation method for several different fuels with an oxygen/air mixture in a different cylindrical chamber. Other publications on experimental works were issued by Wolanski et al. [10] and Kindracki et al. [11]. In numerical studying, research into rotating detonation engine (RDE) combustion has been carried out in Russia, Poland, China, Japan and the USA. Hishida et al. [12] present fundamental information about rotating detonation and Yamada et al. [13] determine the threshold of limit detonation in RDE. Liu et al. [14] achieved detonation combustion under the ramjet inlet (conic combustion chamber). Zhou and Wang [15] presented the paths of flow particles burned by three different processes, which were tracked and analyzed in detail in 2D. The model of the behavior and detonation structure were clearly captured and illustrated. Falempin et al. [16], Mikhailov et al. [17], Schwer et al. [18], Zhdan et al. [19] published many performance results from numerical calculation. Nordeen et al. [20] expressed the thermodynamic equilibrium of rotating detonation. Folusiak et al. [21] used the in-house code “REFLOPS” to represent many numerical calculation results under different chamber configurations and types of mixture in premixed and non- premixed combustion.

2. Numerical calculation results

The selection of an appropriate numerical method and boundary conditions on ANSYS FLUENT are obligatory pre-

*Corresponding author
Email address: jkind@itc.pw.edu.pl (Jan Kindracki)

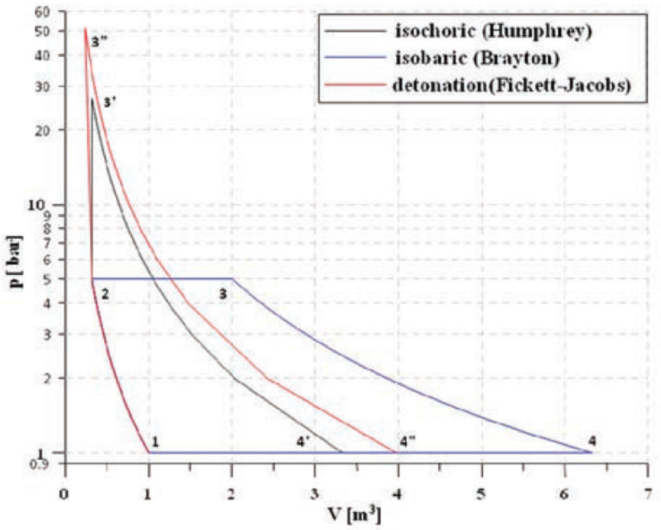

Figure 1: Cross-section plane of the combustion chamber

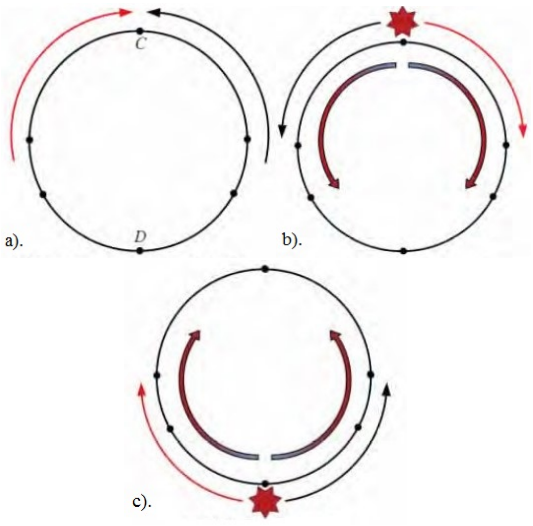

Figure 2: Schematic diagram of counter-direction travelled detonations [12]

requisites for generating successful and reasonable results on simulation of rotating detonation combustion. A density based solver could properly work with a shock wave. The energy equation and standard $k-\varepsilon$ turbulence model were switched on. Furthermore, the density of the medium, and the solution methods prefer the setting "explicit temporal discretization of all solved equations" and "second order numerical scheme" which usually ensure that the detonation wave is not smoothed during calculation. The detailed setting of the boundary conditions will be presented in the following sections.

2.1. Separated injection system

As shown in Fig. 1, we observed that the air and fuel injection systems are independent of each other. The air injection is designed as a narrow slit inlet and fuel injectors consist of a number of orifices. This design concept allows gas to pass through the injection systems under sonic conditions; moreover, the mixing process is sufficient prior to combustion.

2.2. Counter-direction moved detonations

As illustrated in Fig. 2, after successful initiation, two counter-direction moved detonations will be generated. They will impact each other at some points in the chamber and repeat this process until only one detonation survives the collision battle. Usually, the process lasts about $0.3 \sim 20$ ms.

2.3. Simulation results with 40 fuel injectors

After successful initiation, two detonation waves will act as a counter-directional movement. As shown in Fig. 3, the highest pressure is present at the detonation front, which is also detonated as the most energetic part of detonation. Moreover, the shock waves reflection and Mach reflection are expressed behind the detonation front. Those multi-reflected shock waves are formed between the inner and outer chamber surfaces. Easier formation of Mach reflection can be obtained under lower average axial velocity [21].

Illustration of the pressure contour of detonation clearly shows the formation of the shock wave and pressure distribution during detonation propagation. Comparably, the temperature contour could reasonably express the temperature gradient and distribution accompanied with varied pressure. In Fig. 4, the relatively higher temperatures represented concentrate near the middle of the chamber width. Unfortunately, such results cannot be expected after the collision of the two detonations; reactivation cannot successfully appear due to the failure of the refilling process. The unburned fuel-air mixtures will rapidly combust when they touch the hot burned products. The probable reason can be concluded as numerical diffusion and a poor relationship between the fresh mixture refilling time and the duration of detonation propagation. To solve the issue of numerical diffusion, the most effective solutions might be either to increase the grid precision (mesh cell resolution) or to use a multiple mechanism reaction with self-designed CFD software [22]. Before improving our model's mesh resolution, the analysis of grid size was to carry out properly. In FLUENT, under standard $k-\varepsilon$ turbulence model, Y+ value has been given by a suggested range from 30 to 500. Our simulated model in case of 40 fuel injectors shows such value around $200 \sim 250$, which is relatively acceptable. If we decided to improve our mesh resolution to obtain better results, the desired Y+ value need to be taken between $30 \sim 110$, and would reach the best results as such value near 30 as possible. Unfortunately, that would be dramatically increase our mesh cell quantities which lead to a prohibitive long calculation time consuming and requirement of high capability of computational devices. However, due to financial and time constraints on this research, neither of these approaches were feasible. Therefore, to find appropriate boundary conditions for the combustion system, a corrected relationship between the refilling time and detonation propagation time is the only choice left. Extensive

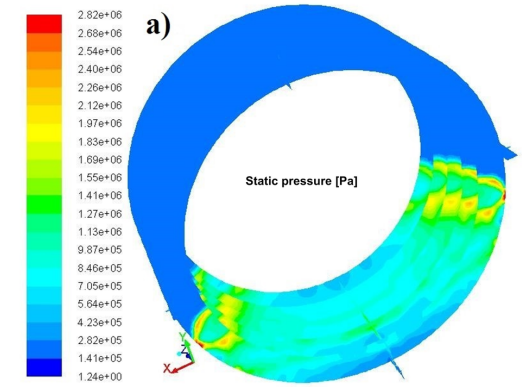

Figure 3: Parameter contours: a) pressure; b) temperature in cross-section planes in the case of 40 fuel injectors

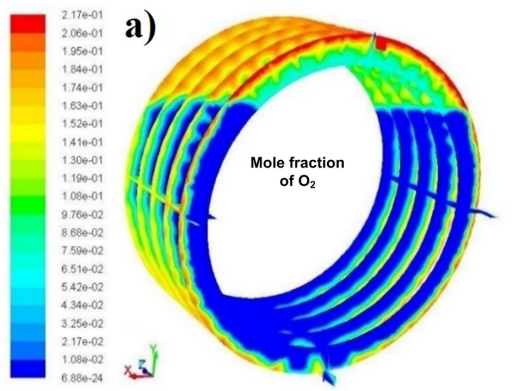

Figure 4: Mole fraction contour: a) oxygen; b) hydrogen in cross-section planes in the case of 40 fuel injectors

experimental experience and theoretical knowledge lent insight into critical factors which determine successful reactivation of detonation and the time of refilling. The correct refilling process/time means that fresh mixture should be injected into the system to ensure the passing through detonation is successfully reactivated after collision. There are generally two approaches: (i) dramatically increase the fresh mixture mass flow rate, which accelerates the injection process, or (ii) keep the same mass flow rate but reduce the detonation propagation velocity (consequently the equivalence ratio must change) which gains extra time for the inflow of unburned gases.

Approach (i) with dramatically increased mass flow rate not only widens the numerical diffusion possibility but also creates a need to rebuild the system boundary conditions to rebalance the stoichiometric equivalence ratio in the new circumstances—all for an unacceptably low efficiency outcome. In contrast, approach (ii) with reduced detonation propagation velocity should theoretically gain significant refilling time without dramatically changing the entire system boundary conditions. Thus, the analyses of hydrogen and oxygen distribution have to be carried out carefully. The corresponding simulation captures are shown as above. The images above clearly show that the hydrogen has local rich conditions; a large amount of hydrogen remained while the oxygen was almost completely burnt out. This is the result of the lower number of fuel injectors that the relatively large pressure requires for each fuel injector if we need to keep the stoichiometric mixture for the entire model. It is also the reason why the detonation instantaneous propagation velocity is faster than the theoretical Chapman-Jouguet velocity, even when the equivalence ratio is equal to 1.

2.4. Simulation results with 80 fuel injectors

By slight decreased Y+ value into range from $180 \sim 230$ in new case (80 fuel injectors model), the mesh cell quantities dramatically increased as we predicted. If we keep similar or greater grid size, the comparison in part of mesh improvement almost meaningless. If we keep same mesh cell quantities, the quality of grid size will getting worse, in other words, the Y+ value will raise some amount which would more or less influence the accuracy of calculation or even tends to unstable of calculation. With comparing above mentioned two approaches with Y+ value in range of $180 \sim 230$, the most effective method to resolve detonation propagation velocity and fresh mixture refilling time issue is by increasing the number of fuel injectors instead of decreasing the fuel injection pressure at each orifice. This approach makes each injector share the entire hydrogen injection pressure down to a small value, while the whole system still maintains the stoichiometric condition. In Fig. 5b, we observe more uniformed temperature distribution and the higher temperature zone tightly follows the driving shock wave. These results are quite close to the theoretical assumptions that the most ener-

getic combustion zone is the detonation front, which contains the largest exothermic reaction release of energy to support the continuous propagation of the shock wave. The better results present as we wished. However, the unstable numerical calculation process frequently reported that the solution tends toward divergence, especially the moment after collision. This may explained by the relatively a little bit coarser mesh near the front part of chamber where the fresh mixture mixes together. However, it is difficult to balance the mesh quantity and quality. With an increased number of fuel injectors, the mesh cells dramatically raised, the computational device either barely runs the calculation or takes a prohibitively long time to work; otherwise, the decreased mesh cells will increase grid size, which drives the instability of calculation.

Unfortunately, the numerous attempts on the model did not deliver successful calculation results without generating a divergence after first collision. The calculations had to be abandoned. However, from the oxygen and hydrogen mole fraction contour, we can see that the local rich mixture condition changes to an almost local stoichiometric condition; after the detonation wave passed, the hydrogen only rarely remained. It proves this approach can be made to work effectively.

2.5. Simulation results with 120 fuel injectors

When the model of 80 fuel injectors was undergoing simulation, the case with a tripled number (120) of fuel injectors was carried out at the same time, for considering both calculation capability and time consuming situation, the third model keep approximate same Y+ value as last case (80 fuel injectors). Comparable results are shown in the form of the images above. Due to the large number of orifices, the hydrogen injection pressure at each injector remains at a very low level if we still keep the same stoichiometric condition as in the original plan for the entire combustion system. The low injection pressure through the fuel injector reverses the local mixture condition from rich to lean. It can be seen from Fig. 6 that the high temperature area is shifted to a position near the chamber outer surface. However, from the analysis of residual unburned mixture, we realize the local stoichiometric combustion condition reverses its situation into a lean state. As was observed, the hydrogen was completely burned out while a large amount of oxygen remained after the detonation wave had passed. These circumstances are much easier for our case (the chamber is relatively small in size) as regards obtaining reactivation and further continuous stable rotating detonation. Nevertheless, the calculation cases with 120 fuel injectors were also abandoned, for the same reason as mentioned in the case of 80 fuel injectors: the calculation had detected unstable error which finally led the results to diverge.

2.6. Simulation results in premixed combustion

Since none of cases delivered the expected successful results under the separation fuel-air injection system (non-premixed mixture), the premixed mixture/combustion had to be developed to achieve the desired goal. By keeping same Y+ value as initial case (Y+ from 200 to 250 in 40 fuel injectors model), the numerical calculation had been carried out. The premixed combustion was able to properly represent the expected results: successful reactivated detonation after collision. The feature and behavior of detonation were recorded, and moreover, the important process of transition from two counter-direction moved detonations to one side single rotating detonation was also captured and logged. These images and data could reasonably explain and express the detonation state, behavior and performance in each of the different stages of propagation. Fig. 7a and Fig. 7b illustrate the detonation front and oblique shock, which are the most characteristic components making up a detonation.

From Fig. 7c we can clearly see that the fresh mixture could be properly injected into the system without immediate combustion upon contact with hot burned products. Moreover, after hundreds of simulations it became clear that the length of the detonation front is mainly determined by the occupation volume of fresh mixture over the entire combustion chamber. In other words, a larger volume fraction of fresh mixture leads to a longer detonation. Thus, a relatively higher mass flow rate was set at the inlet boundary condition to prove our hypothesis. The simulation results are consistent with expectations. However, as the listed captures in Fig. 8 show, there is an extra phenomenon: when a higher mass flow fresh mixture is injected into system, it is very easy to generate a backward detonation during the reactivation process. Backward detonation would mainly lead to two end results. One is backward detonation which remains in the chamber, where the faster consumed unburned mixture makes the original traveled detonation finally transform into deflagration. The other is backward detonation which, after one or a few collisions, will extinguish. Moreover, the most successful and important procedure exhibited by the transition process from a two counter-direction detonation to a one side single rotating detonation was also captured and recorded. It provides important information on how the continuously rotating detonation progressively formed and on what exactly happened at that moment.

From the listed series of captures in Fig. 9, it can be seen that when the collision happens, two passed through detonations would lose some energy during impaction, while during reactivation, they gain energy from the fresh mixture at the current detonation state, which means if one detonation propagates in a relatively low energy state (compared to the other one), during each impaction, the lower energy detonation wave will transform into a “weaker” state than the last moment. This can be understood as a cumulative cycle: the weaker detonation loses more energy, and the greater the energy loss the weaker the detonation during reactivation. This situation will finally lead the low energy detonation wave to disappear because there is too little energy to support further propagation. However, even one side continuously rotating detonation can be successfully generated; it does not mean the detonation will always propagate in a sta-

ble fashion under any kind of boundary condition, there is also a range of boundary conditions which limit the stability of detonation.

With quite fluid boundary conditions, a different detonation structure was obtained. Moreover, a range exists where the detonation propagation was relatively stable when the mass flow rate kept at 0.16 kg/s–0.96 kg/s. While too low a mass flow rate will make reactivation very difficult to achieve, a too high mass flow rate will continuously generate backward detonation, which drags the original detonation into instability. A different mass flow rate will shift the contact surface between the fresh mixture and burned gases. This layer critically influences the length of the detonation front. Meanwhile, the frequently changed boundary condition (mass flow rate) will twist and deform this layer, possibly causing a change in detonation features and making the detonation propagation metastable or even unstable. A different feature of the detonation can be seen in Fig. 10a, b and Fig. 10d. Especially in sub-image Fig. 10d, the oblique shock and shear layer (separating the new combustion products and old burned gas) are combined into one united high temperature zone. It may be caused by the insufficient combustion of the detonation front and the unburned mixture leaking into the territory between the oblique wave and the shear layer generating a secondary combustion. Fig. 10c presents a state of unstable detonation, which is the consequence of frequently changing boundary condition. In this stage, the detonation stays in a state of weak energy propagation, “dormant”. The trigger to wake detonation back to a high energy state is very simple. A sudden change in boundary condition with a relatively large difference in mass flow rate (either increased or decreased, but within the range of stable propagation) or a reset boundary condition to the initial parameter (first successful setting). In the field of numerical calculation, appropriate mesh is always a key factor that not only determines whether the calculation will be successful, but also provides a better representation of the calculation results. With the purpose of gaining a detailed understanding of detonation, a fine mesh model was built (Fig. 11). The high resolution case with improved grid size as taken Y+ value range as $45 \sim 115$, Such value almost reaches the best acceptable condition as it can be with considering all kinds of situations. A higher mesh resolution gives a better representation of the structure of detonation. However, the united high temperature zone which combined the oblique shock and shear layer was also reported in the case of the fine mesh model. As mentioned before, this phenomenon could explained by insufficient combustion of the detonation front, owing to distortion (bending). This may be the result of a change in mass flow rate, which directly shifted the contact surface between the fresh mixture and the old burned gases, and the twisted surface somehow bent the detonation front thereby causing the shear layer to move closer to the oblique shock. The distorted detonation front meant the fresh mixture could not be sufficiently burned, which made the slightly unburned mixture flow into the area between the oblique shock and shear layer thereby causing secondary combustion. Furthermore,

Table 1: Locations of Artificial Pressure Sensors.

	P_1	P_2	P_3	P_4	P_5	P_6
X	0	42.5	42.5	0	-42.5	-42.5
Y	49	24.5	-24.5	-49	-24.5	24.5
Z	20	20	20	20	20	20

Table 2: Calculated detonation propagation velocities in period (α) and (γ)

Chabmer Dimensions: Diameter = 0.1 m, Circumference = 0.31416

Sensor\Period	Period (α) V_{inst}, m/s	Period (γ) V_{inst}, m/s	
P_1	1481.9 1570.8	1492.4	
P_2	1464.6 1559.1	1559.1	
P_3	1532.5 1506.8	1566.9	V_{CJ} = 1627.7 m/s
P_4	1540.0 1551.4	1555.2	
P_5	1532.5 1506.8	1517.7	
P_6	1464.6 1559.1	1478.4	
V_{mean} V_{mean}/V_{CJ}	1541.9 -9.47%	1536.5 -9.44%	

the insufficient combustion reduced the containing energy in the detonation front, less driven energy “dragged” its position further back than it should be, resulting in the feature that the oblique shock was moved parallel with the detonation front. This situation would be sooner or later returned to its “regular” combustion state, but the high temperature zone which united the oblique shock and shear layer may hold until the next change of boundary condition or those two components are quickly separated from each other by the reformation of the detonation front in a regular structure. Apart from direct visual observation of the structure of the detonation wave, another approach to recognize the detonation combustion is to utilize pressure sensors to measure or record the detonation propagation performance and behavior. To do this, several artificial pressure sensors need to be placed near the outer surface of combustion chamber (Fig 12 and Table 1).

As the table above shows, the six pressure sensors are in one plane, offset 20 mm from the inlet in the axial direction (Z direction) of the chamber. Because non-premixed combustion cannot successfully reactivate detonation after collision, the graphs presented below and the calculated propagation velocity table are all based on premixed cases. Calculated detonation propagation velocities in period(α) and (γ).

As observed from Fig. 13a, after successful initiation, three stages usually appeared for an entire combustion. The first stage, two counter-direction moved detonation which denotes as period (α), then period (β) which is the process of transfer from two counter-direction traveled detonation to one side single rotating detonation, the last stage is period (γ) which is the formation of stable one side rotating detonation. The measured pressures in period (α) are generally higher than period (γ), this is because of the huge increase

of pressure magnitude during impaction and also a relatively larger mass flow rate was set as the initial boundary condition, which meant the detonation front had been elongated through the whole chamber axial length during reactivation. In other words, due to the large mass flow rate injected into the chamber (chamber axial length only 50 mm), there was no place to allow the formation of oblique shock. The calculated detonation velocities were not presented in period (β) because detonation propagation in this process is unpredictable and incalculable. The duration of this process can be typically from 0.1 ms to 20 ms (experiment value from Kindracki [23]), and it is good that in our calculation it only took 0.25 ms. As we mentioned, the mass flow rate in period (α) was larger than the last period (six times higher than in period (γ)). For the purpose of determining the detonation structure, behavior and performance, we progressively decrease the mass flow rate. The detonation front shortened as expected and oblique shock was also observed at period (γ) when stable one side rotating detonation was represented. Table 2 gives the calculated detonation velocities. Those velocities are actually instantaneous velocities (Vinst) which are calculated as a ratio of detonation wave displacement through two certain defined positions of sensors. Those calculated velocities provide information on how fast the detonation wave was propagating during different times, moreover, mean velocity Vmean also needs to be expressed with reference to the general detonation propagation state in each period. By comparing two groups of values of velocity, it is apparent that the detonation traveling velocity did not fluctuate very much, instead remaining at a relatively constant level during propagation, and that level is directly connected with the composition of the fresh mixture. Theoretical (Chapman-Jouguet) velocity is ideal detonation propagation velocity. By comparing the obtained/calculated results, the velocity deficit during propagation was determined. However, due to the fixed sensor locations, those artificial sensors actually recorded the pressure magnitudes at the oblique shock part, leaving the detonation front data unrecorded at that moment. To explore all aspects of analysis of detonation performance and behavior, two groups of sensors with different axial locations were used. The second group of sensors was aligned with the previous ones in parallel cross-section plane, but shifted forward 10 mm in the axial (Z) direction. In other words, the same XY position as in the previous sensor locations, but moved closer (10 mm offset from the inlet) to the inlet of the chamber. This rearrangement ensured correct pressure measurements of the detonation front within a reasonable range of mass flow rate. To immediately observe one side rotating detonation after initiation, a complex approach was applied in our model during the initiation of detonation. We inserted an artificial wall near the patch zone, and this wall halved the chamber into two equal parts. During initiation, a huge amount of energy was released from the patch zone, and detonation wave was able to propagate in any direction inside the chamber. Excluding the waves, flowing out of the chamber through inlet and outlet, there were two main detonation trajectories of interest. One was a detonation propagating far away from the middle wall, and the other one was traveling in the opposite direction, moving forward to the wall. The one heading toward to the wall was reflected when it hit the solid surface, but this wave disappeared more quickly because there was no fresh mixture to support the reflected detonation. Thus, one side single rotating detonation was quickly obtained (middle wall switched back to fluid state while the reflected detonation disappeared). Fig. 14 shows stable rotating detonation immediately after the initiation. The measured detonation front peak pressure (in Fig. 14b) is much higher than the oblique shock part (in Fig. 14a). This is because the detonation front is the most energetic part driving the whole detonation propagation and the oblique shock is the accompanying component when the detonation front contacts the old burned gases. However, pressure measurement from the oblique shock could more clearly deliver information on the state of detonation changes. The pressure measurement in Fig. 14a shows a “block” like pattern: each block has similar peak pressure and then shifts its amplitude almost entirely higher or lower. This is the result of a change in magnitude of the mass flow rate and the duration of change under such boundary conditions. For instance, a higher block means a relatively larger mass flow rate which results from elongating the detonation front, and a wider block tells us how much time the detonation propagated under that boundary condition. Quite frequently a change in mass flow rate will make a state of detonation propagation unstable. As shows on Fig. 14a and Fig. 14b, there was a moment where the recorded peak pressure remained at a very low level. As explained earlier, the reason was mainly caused by the twisted and deformed contact surface which directly affected the stable propagation of detonation. The unstable detonation combustion released very low energy, which made the detonation itself enter a “dormant” like state. In this state, detonation was not completely extinguished, but propagated very weakly. The trigger to “wake up” detonation is to reset the mass flow rate.

The traveling velocities were quite close to the theoretical value (V_{CJ}) in the case of “forced” one side rotating single detonation propagation in part of the calculated propagation velocities. This was the result of not only no more energy loss during collision and/or reactivation, but also of the use of finer mesh which delivers a more accurate solution. Nevertheless, the calculation was based on the visible peak pressures, the velocity during weak detonation propagation was not calculable, but experimental experience and theoretical knowledge suggested very strongly that the detonation at that moment traveled at relatively low speed (e.g. calculated velocity at pressure sensor P4 and P10 provided information that at some moments detonation propagation velocity dropped to below 1500 m/s which caused a 10.7% loss of velocity in respect of V_{CJ}).

Table 3: Calculated detonation propagation velocities in forced one side rotating single detonation (for next passes of the wave)

Chamber Dimensions: Diameter = 0.1 m, Circumference = 0.31416				
	V_{inst}, m/s		V_{inst}, m/s	
	1707.4		1750.2	
	1764.9		1764.9	
P_1	1726.2	P_7	1730.9	
	1640.5		1649.1	
	1503.2		1496.0	
	1481.9		1485.4	
	1716.7		1721.4	
	1779.9		1785.0	
P_2	1716.7	P_8	1716.7	
	1657.8		1662.2	
	1510.4		1517.7	
	1689.0		1816.0	
	1842.6		1671.1	
P_3	1657.8	P_9	1735.7	
	1726.2		1510.4	
	1496.0		1503.2	
	1716.7		1810.7	V_{CJ} = 1679.9 m/s
	1760.0		1671.1	
P_4	1689.0	P_{10}	1779.9	
	1805.5		1536.2	
	1492.4		1496.0	
	1875.6		1785.0	
	1721.4		1716.7	
P_5	1662.2	P_{11}	1662.2	
	1657.8		1666.6	
	1506.8		1506.8	
	1764.9		1760.0	
	1740.5		1745.3	
P_6	1707.4	P_{12}	1712.0	
	1636.2		1640.5	
	1503.2		1503.2	
V_{mean}	1675.6		1666.6	
V_{mean}/V_{CJ}	-0.25%		-0.8%	

3. Summary and Conclusion

When engaged in the numerical calculation of rotating detonation, involving a range of simulation models, various conditions are vital for successful results. The obligatory conditions which strongly constrain stable detonation generation and propagation are the chamber configurations and its relative boundary conditions. From extensive investigation and research, stable rotating detonation would hardly take place with a rich hydrogen-air mixture due to insufficient time for refilling. The approach to solve such problem is either to replace the model with a larger size chamber or to reset a low composition of mixture with a higher mass flow rate into boundary conditions. In this study, the small size chamber was fixed all the time, thus, to obtain stable rotating detonation in a relatively short time, a lean mixture with a slightly higher mass flow rate was necessary. Unfortunately, non-premixed combustion did not allow the refilling process to be achieved through the use of a separate injection system due to the huge gradients of inlet parameters (e.g. significant differences between flow velocity, density and pressure). The premixed combustion model with comparable inlet boundary conditions was tested as a substitution. After successful simulation in (i) two counter-direction moved detonation waves and (ii) a one side rotating single detonation wave, it was found that it is much easier to achieve stable rotating detonation with a lean fuel mixture than with a stoichiometric or rich fuel mixture. Coarse and unstructured mesh could generate inappropriate and unreasonable results. In non-premixed combustion, numerical diffusion can be related to two reasons. One reason is due to the large size of grids. This issue could be solved by utilizing hexahedron feature structured mesh and by squeezing the grid size into a small dimension near the mixing zone. However, under such a high resolution of grids, the number of cells dramatically increased. Such a complicated model (non-premixed combustion) needs a prohibitively large number of cells to guarantee a lower probability of numerical diffusion. The other reason is the simplification of the combustion reaction. The hydrogen property is very active, under a large size of grid. If the chemical reaction constraint is wrong, the incoming hydrogen will immediately burned as deflagration combustion. Furthermore, the mesh cells and numerical methods can influence the accuracy of simulation results and consuming of calculation time. However, having achieved stable rotating detonation in premixed combustion, it was concluded that in non-premixed combustion model stable rotating detonation could be formed if reactivation can be successfully generated after an appropriate refilling process. Successful detonation in premixed combustion was carried out in many kinds of different cases and situations, with different structure of detonations expressed. Finally, a range of mass flow rate was determined that could generate a detonation wave and would not influence detonation propagation too much and thereby directly cause unstable combustion. Furthermore, frequently changed mass flow rate twisted the contact surface, triggering a series of changes at the detonation front and oblique shock, and the metastable detonation combustion could be easily transferred into uncoupled detonation. However, that state could reverse very rapidly to detonation combustion automatically after a few hundred microseconds. Alternatively, it barely happened as the manually reset boundary condition combined with a sudden huge different mass flow rate to force reformation of a new detonation, otherwise, the uncoupled unstable detonation would completely transform into deflagration—then the only option left is to start initiation again. Numerical simulation of 3D rotating detonation is difficult. It requires great knowledge of both theoretical and numerical elements, the proper CFD tools and computational device and a good deal of patience. The numerical simulation in this study is but one small step and much more analysis is needed in this field. More detailed structure and combinative behaviors (such as pressure, temperature and velocity) of detonation could be delivered in future research. Regardless of how the combustion engine industry evolves, the authors strongly believe that it is only a matter of time before detonation combustion will be the predominant technology in future jet engine systems.

Acknowledgments

The authors would like to thank Arkadiusz Kobiera, Piotr Wolanski and Sławomir Kubacki for their many fruitful and valuable discussions during this study.

References

[1] D. L. Chapman, Vi. on the rate of explosion in gases, The London, Edinburgh, and Dublin Philosophical Magazine and Journal of Science 47 (284) (1899) 90–104.

[2] E. Jouguet, Sur la propagation des réactions chimiques dans les gaz, J. Math. Pures Appl 1 (1905) 347–425.

[3] B. V. Voitsekhovskii, V. V. Mitrofanov, M. E. Topchiyan, Structure of the detonation front in gases, Izdatielstvo SO AN SSSR.

[4] J. A. Nicholls, H. R. Wilkinson, R. B. Morrison, Intermittent detonation as a thrust-producing mechanism, Journal of jet propulsion 27 (5) (1957) 534–541.

[5] A. Tobita, T. Fujiwara, P. Wolanski, Detonation engine and flying object provided therewith, uS Patent 7,784,267 (Aug. 31 2010).

[6] F. A. Bykovskii, V. V. Mitrofanov, E. F. Vedernikov, Continuous detonation combustion of fuel-air mixtures, Combustion, Explosion and Shock Waves 33 (3) (1997) 344–353.

[7] F. A. Bykovskii, S. A. Zhdan, E. F. Vedernikov, Continuous spin detonation in annular combustors, Combustion, Explosion, and Shock Waves 41 (4) (2005) 449–459.

[8] F. A. Bykovskii, S. A. Zhdan, E. F. Vedernikov, Continuous spin detonation of hydrogen-oxygen mixtures. 1. annular cylindrical combustors, Combustion, Explosion, and Shock Waves 44 (2) (2008) 150–162.

[9] F. A. Bykovskii, E. F. Vedernikov, Continuous detonation of a subsonic flow of a propellant, Combustion, Explosion, and Shock Waves 39 (3) (2003) 323–334.

[10] P. Wolanski, J. Kindracki, T. Fujiwara, An experimental study of small rotating detonation engine, Pulsed and continuous detonations (2006) 332–338.

[11] J. Kindracki, P. Wolanski, Z. Gut, Experimental research on the rotating detonation in gaseous fuels–oxygen mixtures, Shock waves 21 (2) (2011) 75–84.

[12] M. Hishida, T. Fujiwara, P. Wolanski, Fundamentals of rotating detonations, Shock waves 19 (1) (2009) 1–10.

[13] T. Yamada, K. Hayashi, N. Tsuboi, E. Yamada, V. Tangirala, T. Fujiwara, Numerical analysis of threshold of limit detonation in rotating detonation engine, in: 48th AIAA Aerospace Sciences Meeting Including the New Horizons Forum and Aerospace Exposition, 2010, p. 153.

[14] S. Liu, Z. Lin, W.-D. Liu, W. Lin, Research on continuous rotating detonation wave propagation process (ii): Two-wave collision propagation mode, Tuijin Jishu/Journal of Propulsion Technology 35 (2) (2014) 269–275.

[15] R. Zhou, J.-P. Wang, Numerical investigation of flow particle paths and thermodynamic performance of continuously rotating detonation engines, Combustion and Flame 159 (12) (2012) 3632–3645.

[16] F. Falempin, E. Daniau, N. Getin, F. Bykovskii, S. Zhdan, Toward a continuous detonation wave rocket engine demonstrator, in: 14th AIAA/AHI Space Planes and Hypersonic Systems and Technologies Conference, 2006, p. 7956.

[17] V. Mikhailov, M. Topchiyan, Studies of continuous detonation in an annular channel, Fizika Goreniya I Vzryva 1 (4) (1965) 20–23.

[18] D. Schwer, K. Kailasanath, Numerical study of the effects of engine size n rotating detonation engines, in: 49th AIAA Aerospace Sciences Meeting including the New Horizons Forum and Aerospace Exposition, 2011, p. 581.

[19] S. A. Zhdan, A. M. Mardashev, V. V. Mitrofanov, Calculation of the flow of spin detonation in an annular chamber, Combustion, Explosion, and Shock Waves 26 (2) (1990) 210–214.

[20] C. Nordeen, D. Schwer, F. Schauer, J. Hoke, B. Cetegen, T. Barber, Thermodynamic Modeling of a Rotating Detonation Engine, in: 49th AIAA Aerospace Sciences Meeting including the New Horizons Forum and Aerospace Exposition, Aerospace Sciences Meetings, American Institute of Aeronautics and Astronautics, 2011. doi:doi:10.2514/6.2011-803.
URL http://dx.doi.org/10.2514/6.2011-803

[21] M. Folusiak, A. Kobiera, P. Wolanski, Rotating detonation engine simulations in-house code-reflops, Prace Instytutu Lotnictwa (2010) 3–23.

[22] J. Wang, Research progress on crde at peking university, Tech. rep., Center for Combustion and Propulsion. Peking University (2009).

[23] J. Kindracki, Badania eksperymentalne i symulacje numeryczne procesu wirującej detonacji gazowej, Ph.D. thesis, Warsaw University of Technology (2008).

Table .4: Boundary conditions for premix cases

	Inlet	Outlet
Total pressure, Pa	223448	217800
Total temperature, K	366	290
Species:		
H2	0.015	-
O2	0.232	-
N2	0.753	-

Table .5: Boundary conditions for non-premix cases

	Air inlet	H2 inlet	Outlet
Total pressure, Pa	223448	550000	217800
Total temperature, K	366	305	290
Species:			
H2	-	1	-
O2	0.232	-	-
N2	0.768	-	-

Appendix A

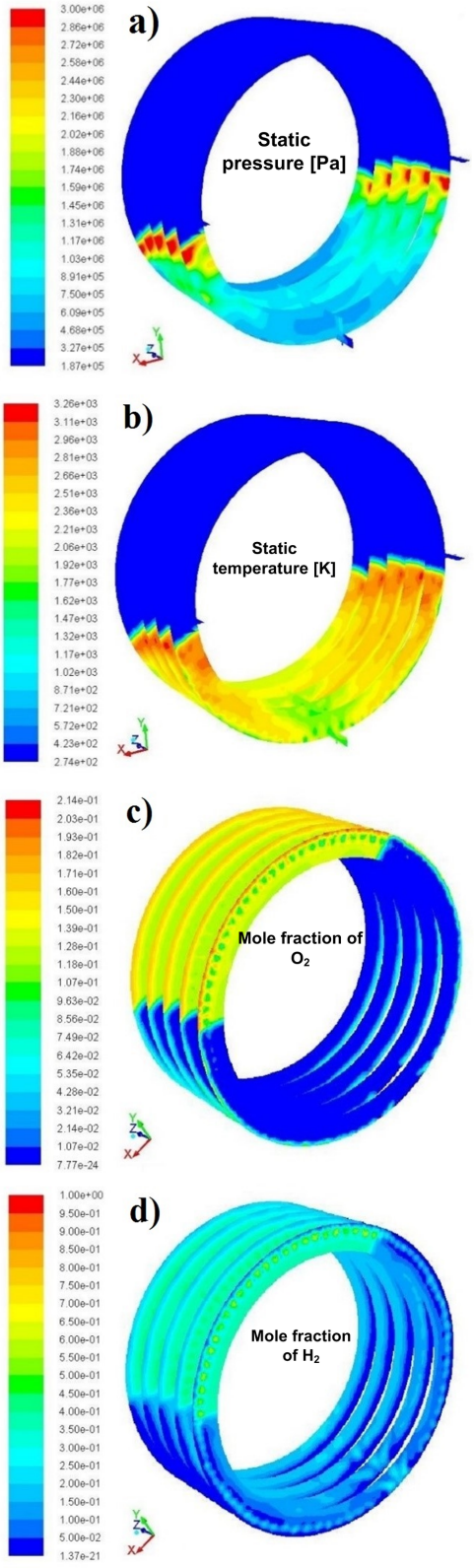

Figure 5: Parameters contours: a) pressure; b) temperature; c) oxygen mole fraction; d). hydrogen mole fraction in cross-section planes in the case of 80 fuel injectors

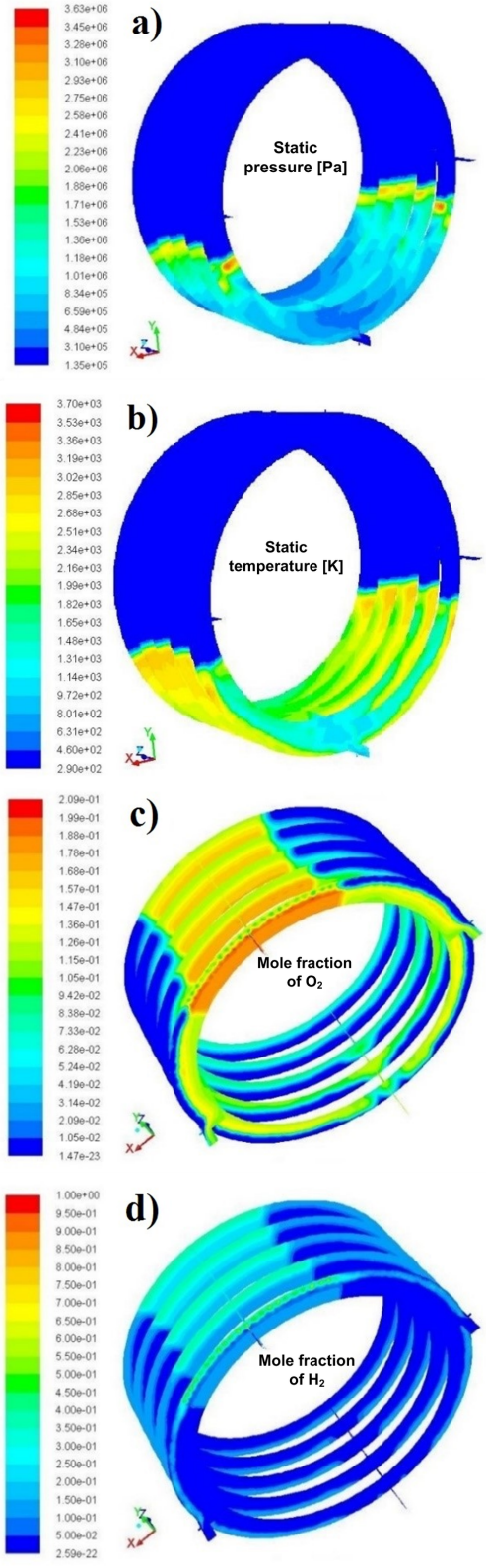

Figure 6: Parameters contours: a) pressure; b) temperature; c) oxygen mole fraction; d) hydrogen mole fraction in cross-section planes in the case of 120 fuel injectors

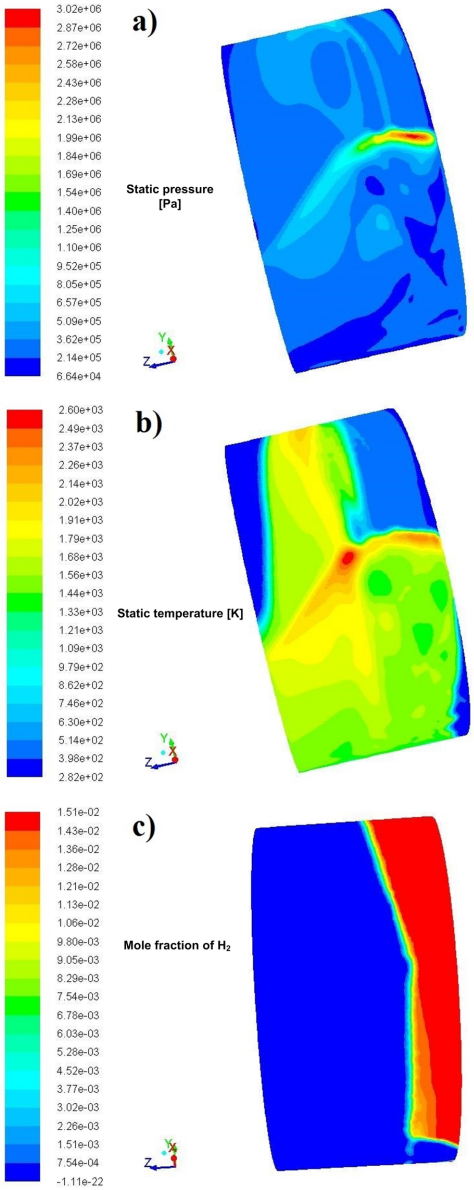

Figure 7: Parameter contours: a) pressure contour; b) temperature contour; c) hydrogen mass fraction contour in outer surface in premixed combustion

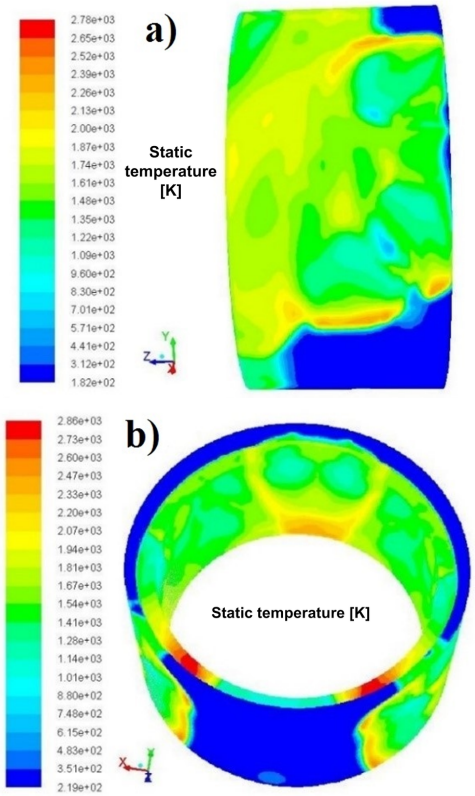

Figure 8: Temperature contour: a) at outer surface; b) in isometric view with massive increased mass flow rate

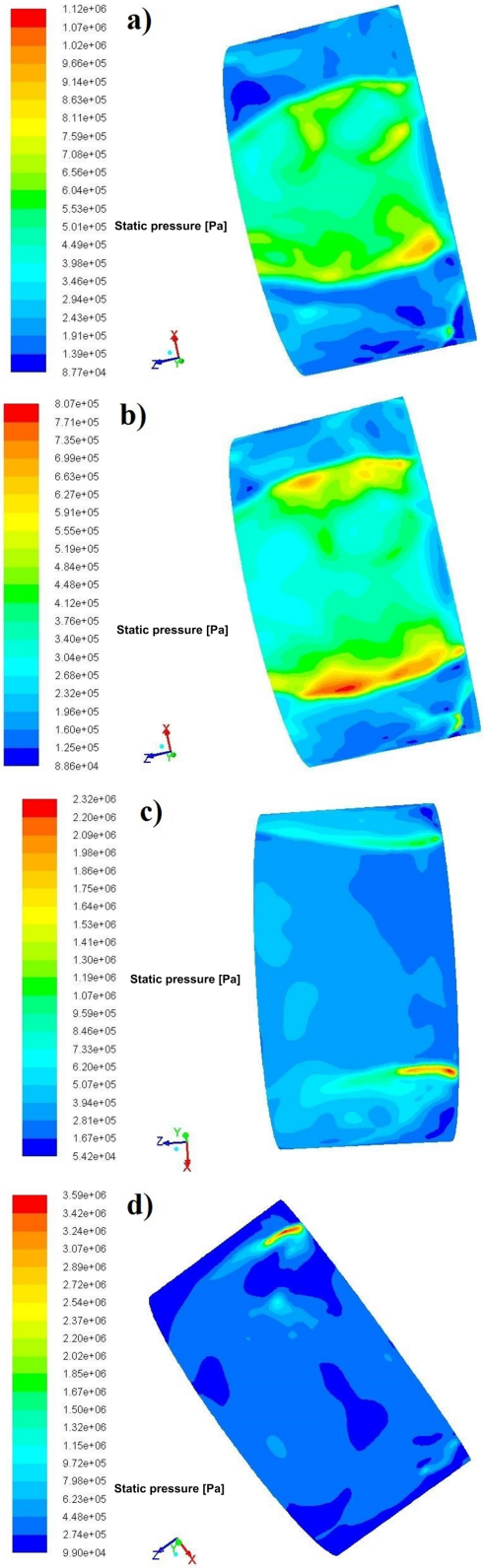

Figure 9: Pressure contour of transition process a) at 644.5 μs (outer surface); b) at 648 μs (outer surface); c) at 720.5 μs (outer surface); d) at 942 μs (outer surface); e) at 985 μs (isometric view)

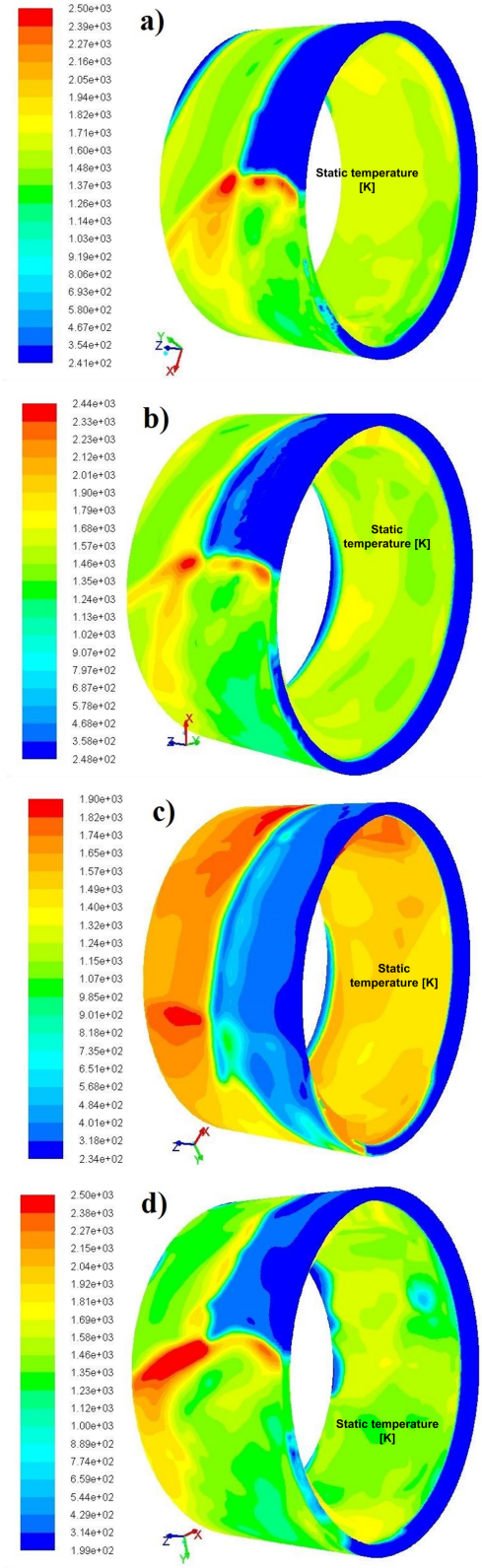

Figure 10: Temperature contour within range of mass flow rate 0.32 kg/s–0.48 kg/s. Detonation propagation (isometric view): a) at 1.038 ms; b) at 1.1645 μs; c) at 1.5435 ms; d) at 2.3105 ms

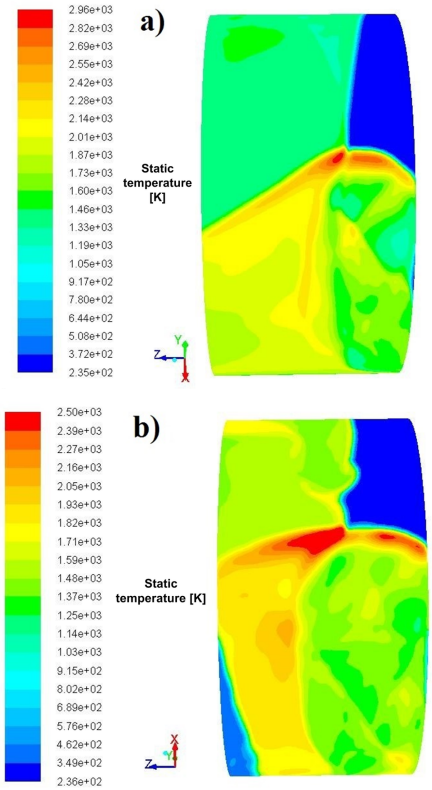

Figure 11: Temperature contour of detonation structure with different mass flow rate in fine mesh model. Detonation propagation (outer surface) a) propagation at 271 μs; b) propagation at 409.5 μs

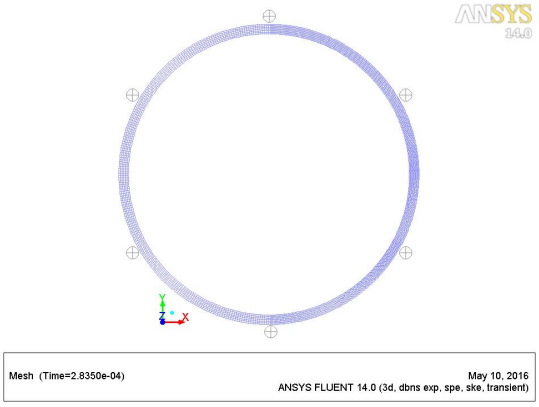

Figure 12: Locations of artificial pressure sensors in axial view.

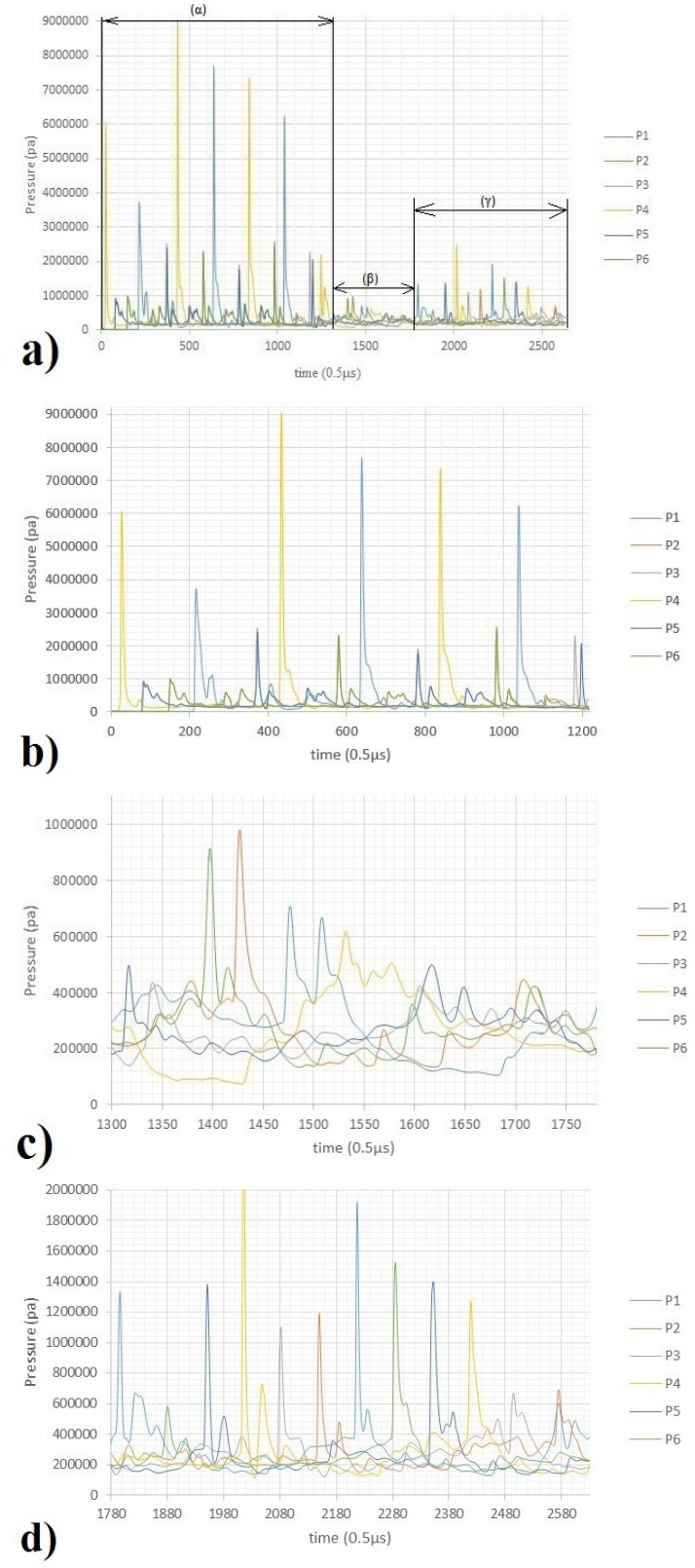

Figure 13: Pressure measurements in premixed combustion under different boundary conditions: a) entire results; b) period (α); c) period (β); d) period (γ)

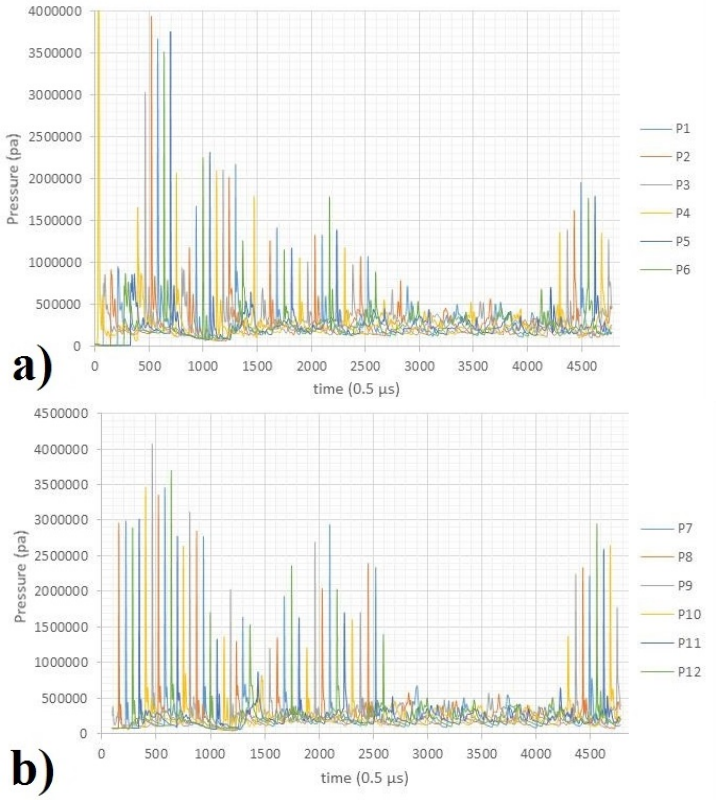

Figure 14: .Pressure measurements of: a) oblique shock; b) detonation front in the case of forced one side rotating detonation in premixed combustion